



## Electronic properties of freestanding $\text{Ti}_3\text{C}_2\text{T}_x$ MXene monolayers

A. Miranda,<sup>1</sup> J. Halim,<sup>2,3</sup> M. W. Barsoum,<sup>2</sup> and A. Lorke<sup>1</sup>

<sup>1</sup>Department of Physics, Universität Duisburg-Essen, Duisburg 47058, Germany

<sup>2</sup>Department of Materials Science and Engineering, Drexel University, Philadelphia, Pennsylvania 19104, USA

<sup>3</sup>Thin Film Physics Division, Department of Physics, Chemistry and Biology (IFM), Linköping University, SE-581 83 Linköping, Sweden

(Received 9 November 2015; accepted 28 December 2015; published online 19 January 2016)

We report on the electrical characterization of single MXene  $\text{Ti}_3\text{C}_2\text{T}_x$  flakes (where T is a surface termination) and demonstrate the metallic nature of their conductivities. We also show that the carrier density can be modulated by an external gate voltage. The density of free carriers is estimated to be  $8 \pm 3 \times 10^{21} \text{ cm}^{-3}$  while their mobility is estimated to be  $0.7 \pm 0.2 \text{ cm}^2/\text{V s}$ . Electrical measurements, in the presence of a magnetic field, show a small, but clearly discernable, quadratic increase in conductance at 2.5 K. © 2016 AIP Publishing LLC. [<http://dx.doi.org/10.1063/1.4939971>]

Since the discovery of graphene,<sup>1,2</sup> there has been a growing, and renewed, interest in a wide variety of two-dimensional (2D) materials, such as hexagonal BN,<sup>3</sup>  $\text{MoS}_2$ ,<sup>4</sup>  $\text{WSe}_2$ ,<sup>5</sup> among many others, because of their promising properties that can be exploited for numerous applications. Recently, MXenes—2D early transition metal carbides and carbonitrides—have been produced by the selective etching of the A layers from the MAX phases.<sup>6</sup> The latter is a large family of layered compounds, with the general formula  $\text{M}_{n+1}\text{AX}_n$  ( $n = 1-3$ ), where M is an early transition metal, A is an A-group element (mostly groups 13 and 14), and X represents C or N.<sup>7</sup> More than 70 MAX phases are known to exist<sup>8</sup> and they have led to numerous technical applications,<sup>9</sup> owing to their unique combination of both metallic and ceramic properties,<sup>10,11</sup> as well as their favorable mechanical,<sup>12</sup> thermal,<sup>13</sup> and chemical<sup>14</sup> characteristics.

The vast majority of MXenes known to date have been produced by selectively etching Al from Al-containing MAX phases.<sup>15</sup> During the etching process, the MXene surface acquires terminating functional groups, which is why they are commonly designated as  $\text{M}_{n+1}\text{X}_n\text{T}_x$ , where  $\text{T}_x$  represents surface terminating groups such as  $-\text{O}$ ,  $-\text{OH}$ , and/or  $-\text{F}$ .<sup>16-18</sup> MXenes have already been demonstrated to be promising candidates for energy storage applications such as Li-ion batteries,<sup>17,19</sup> Li-S batteries,<sup>20</sup> non-Li-ion batteries such as Na, K, and Ca-ion batteries,<sup>21</sup> electrochemical supercapacitors,<sup>18,22,23</sup> and fuel cells.<sup>24</sup> Apart from the energy storage applications, MXenes were tested as photocatalytic material,<sup>25</sup> gas sensors,<sup>26</sup> biosensors,<sup>27</sup> transparent, conductive electrodes,<sup>28</sup> and for water treatment.<sup>29</sup>

The purpose of this work is to report on the electrical properties of  $\text{Ti}_3\text{C}_2\text{T}_x$  monolayers in the 2.5 K to 300 K temperature range. Herein, we show that individual  $\text{Ti}_3\text{C}_2\text{T}_x$  flakes exhibits metallic behavior. Furthermore, as we demonstrate here, they may be promising for electronic applications, such as metallic, transparent coatings, or even field-effect devices. The influence of a magnetic field on the conductivity was also studied. While the room temperature results indicate promising properties for applications, the low-temperature measurements reveal intriguing characteristics, which can be attributed to the peculiar band structure and the 2D nature of this MXene.

Powders of  $\text{Ti}_3\text{C}_2\text{T}_x$  were produced by adding  $\text{Ti}_3\text{AlC}_2$  powders to a premixed aqueous solution of HCl and LiF in an ice bath. After rinsing in HCl, LiCl, and water, and vacuum filtering, the obtained  $\text{Ti}_3\text{C}_2\text{T}_x$  flakes are similar to those of other MXenes, as shown in supplementary Figure S1(a). The flakes were dispersed in deaerated, distilled water (for more details of MXene production, see the supplementary material<sup>30</sup>).

In order to create the electronic devices, the solution was diluted in ethanol (1:6 by volume) and drop-cast on  $6 \times 6 \text{ mm}^2$  sized silicon substrates, covered with 300 nm of thermally grown  $\text{SiO}_2$ . After an initial pre-annealing step to remove adsorbed water, contacts on monolayer MXene flakes were fabricated by electron beam lithography and deposition of 5 nm/110 nm Ti/Au layers as shown in supplementary Figure S1(b). Immediately after fabrication, the sample was annealed again, wire-bonded, and inserted in a vacuum chamber (details of the device fabrication can be found in supplementary material<sup>30</sup>).

An initial electrical characterization was carried out by sweeping the source-drain voltage,  $V_D$ , between  $\pm 1 \text{ V}$  and recording the resulting current,  $I$ , at various temperatures, in the 2.5 K to 300 K temperature range. Fig. 1 shows typical I-V curves obtained at 300 K and 2.5 K. At 300 K, an Ohmic regime is observed with a constant sheet resistance of  $\rho = 13.6 \text{ k}\Omega/\square$ . At 2.5 K, the I-V curve is slightly nonlinear with a  $V_D$ -dependent differential sheet resistance of  $17.8 \text{ k}\Omega/\square$ ,  $15.3 \text{ k}\Omega/\square$ , and  $14.3 \text{ k}\Omega/\square$  at drain voltages of 0 V, 0.5 V, and 1 V, respectively. The inset in Fig. 1 shows the temperature dependence of the measured sheet resistances at  $V_D = 0.5 \text{ V}$ . With decreasing temperature, the resistance first decreases until about 250 K and then increases slightly all the way down to 2.5 K. We attribute the small increase in resistance ( $\approx 12\%$ ) at the lower temperatures mainly to contact resistance effects.

Using the Si substrate as a backgate electrode, the field-effect of a typical  $\text{Ti}_3\text{C}_2\text{T}_x$  flake was investigated by sweeping the backgate voltage,  $V_G$ , between  $\pm 80 \text{ V}$ , while keeping  $V_D$  fixed at  $+0.5 \text{ V}$ . As can be observed in Fig. 2(a), at 300 K, the drain current,  $I_D$ , shows a linear increase with increasing  $V_G$ . This is a clear indication that the sample exhibits  $n$ -type conductivity.

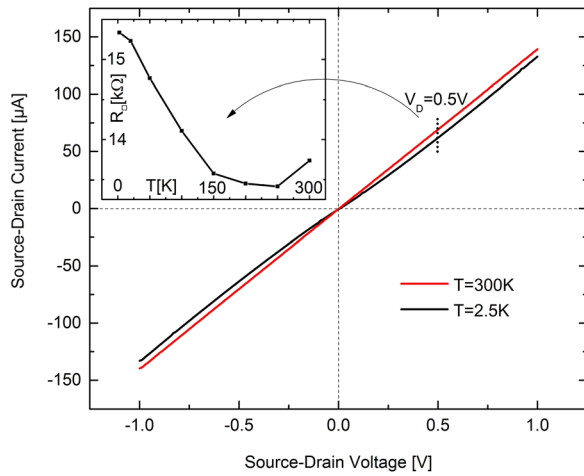


FIG. 1. I-V curve of a monolayer  $\text{Ti}_3\text{C}_2\text{T}_x$  flake at 300 K and 2.5 K showing metallic behavior. The slight non-linearity at 2.5 K is probably due to contact resistance. The inset shows the temperature dependence of the sheet resistance for a drain voltage of 0.5 V. The sheet resistance has a minimum at 250 K and increases by  $\approx 12\%$  as the temperature is decreased.

From a linear fit of the data, the field effect mobility can be determined from the standard relation

$$\mu = \frac{\Delta\sigma}{e\Delta n} = \frac{\Delta I_D}{\Delta V_G} \frac{t}{\epsilon\epsilon_0 V_{SD}} \frac{L}{W}, \quad (1)$$

where  $e$  is the electron charge,  $t$  and  $\epsilon$  are the thickness and permittivity of the  $\text{SiO}_2$  layer,  $\epsilon_0$  is the vacuum permittivity,  $L$  and  $W$  are the length and width of the MXene device, and  $\Delta\sigma$  and  $\Delta n$  are the changes in conductivity and carrier density, respectively. Based on the results shown in Fig. 2(a), a room temperature mobility  $\mu = 0.6 \text{ cm}^2/\text{V s}$  is calculated.

From  $\sigma = \mu n_0 e$ , we calculate an electron density  $n_0$  in  $\text{Ti}_3\text{C}_2\text{T}_x$  of  $7.5 \times 10^{14} \text{ cm}^{-2}$ . Taking the thickness of a single layer  $\text{Ti}_3\text{C}_2\text{T}_x$  flake to be 0.75 nm,<sup>31</sup> the volume density is estimated to be  $1 \times 10^{22} \text{ cm}^{-3}$ , in reasonable agreement with the value of  $3.1 \pm 0.7 \times 10^{22} \text{ cm}^{-3}$ , obtained from electrical measurements on spincoated  $\text{Ti}_3\text{C}_2\text{T}_x$  films<sup>32</sup> and theoretical predictions.<sup>31,33</sup> The average mobility and carrier density, obtained from several investigated samples are  $\mu = 0.7 \pm 0.2 \text{ cm}^2/\text{V s}$  and  $n_0 = 8 \pm 3 \times 10^{21} \text{ cm}^{-3}$ . From control experiments, using a 4-probe geometry, we conclude that the contact resistances do not play a significant role in these measurements.

Figure 2(b) shows the results of the field-effect measurements at 2.5 K. In this case, we observe a clear and abrupt change in slope of the conductance at  $V_{G0} = 18 \text{ V}$ . The region  $V_G < V_{G0}$  can be linearly fitted, from which a field-effect mobility of  $0.2 \text{ cm}^2/\text{V s}$  is calculated. Similarly, the mobility in region  $V_G > V_{G0}$  is calculated to be  $0.8 \text{ cm}^2/\text{V s}$ . Similar changes in slope are observable up to temperatures as high as 200 K. Since  $\sigma = \mu n e$ , such a distinct change in transconductance  $d\sigma/dV_G$  can only have two origins: An abrupt change in capacitance or an abrupt change in mobility. The former can be ruled out as the capacitance is given by the thickness of the  $\text{SiO}_2$  layer and because the same substrates have been used by us for graphene field-effect devices and have never shown any abrupt changes in capacitance. The change in slope can thus be traced back to changes in

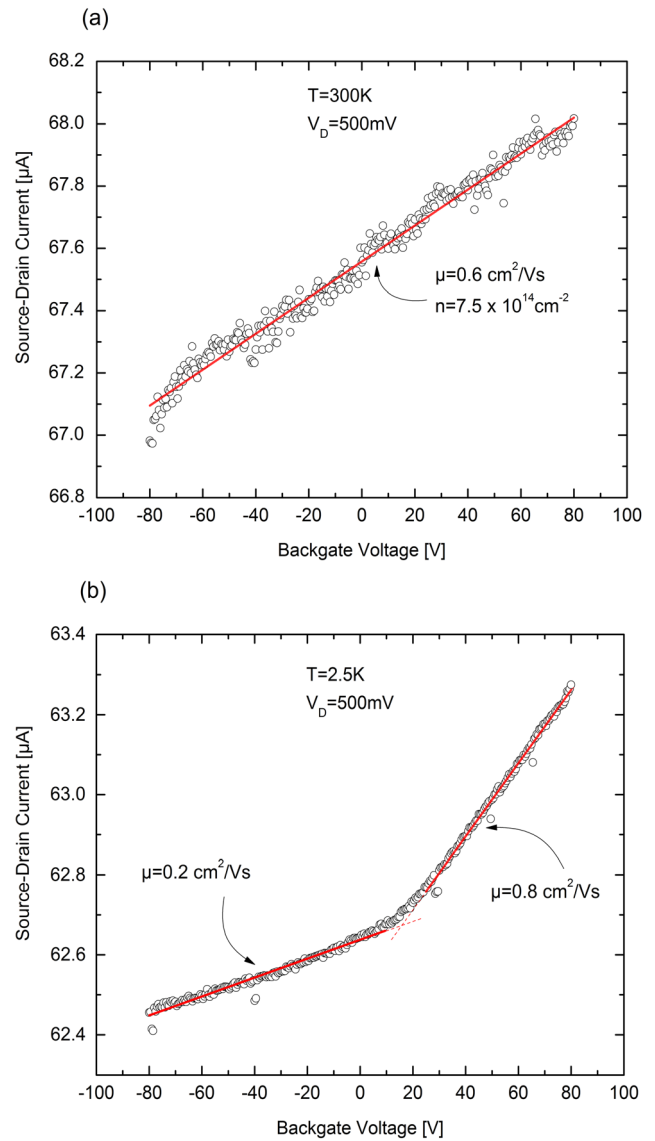


FIG. 2. Functional dependence of source-drain current—for a constant source drain voltage of 0.5 V—on backgate voltage at (a) 300 K and (b) 2.5 K.

either the scattering time,  $\tau$ , or the effective mass  $m_{eff}$ , because  $\mu = e\tau/m_{eff}$ . Therefore, a possible explanation would lie in a multi valley band structure of  $\text{Ti}_3\text{C}_2\text{T}_x$ .

In 2D semiconductor systems, such as Si(100) MOSFETs, it has long been known that a carrier density-dependent, multi-valley occupation can lead to changes in  $m_{eff}$  (and thus in mobility) as a function of  $V_G$ .<sup>34</sup> Multi-valley transport has also been observed in other 2D materials, such as  $\text{WSe}_2$ .<sup>35</sup> More importantly, it was suggested in order to explain the electronic properties of some MAX phases, such as  $\text{Ti}_2\text{AlC}$ .<sup>36</sup> The abrupt change in slope could therefore be qualitatively explained by an occupation of a new set of valleys at  $V_{G0}$ , with a lower mass and/or higher degeneracy. More experimental data, together with detailed band structure calculations—that are beyond the scope of this study—of  $\text{Ti}_3\text{C}_2\text{T}_x$  are needed to further support this model.

Finally, we consider the effects of magnetic fields on the transport properties. As shown in Fig. 3, there is a small, but clearly visible, quadratic increase of the conductance with increasing magnetic field at 2.5 K. As previously observed,<sup>28</sup>

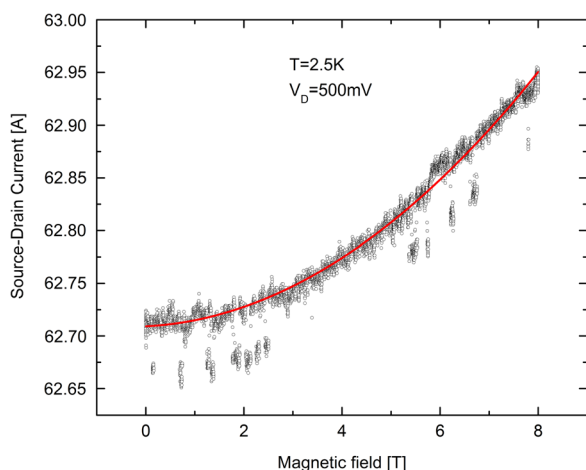


FIG. 3. Effect of magnetic fields on drain currents at a drain voltage of 0.5 V at 2.5 K.

however, the quadratic magneto-conductivity vanishes at temperatures above  $\approx 175$  K (not shown here). These samples did not exhibit effects of weak localization or Shubnikov-de Haas oscillations, presumably because of the low carrier mobilities.

In summary, we investigated the electronic transport and field effects of freestanding, single-layers of  $\text{Ti}_3\text{C}_2\text{T}_x$  in the 2.5 K to 300 K temperature range. The single flakes exhibit metallic electrical conduction. Upon application of a gate voltage, a small but clear field effect was observed, which made it possible to determine the field-effect mobilities, as well as, the carrier-densities. A relatively low mobility of  $\approx 1 \text{ cm}^2/\text{V s}$  was found; the corresponding carrier densities were  $\approx 5 \times 10^{14} \text{ cm}^{-2}$ . Also, a small but clearly discernable, quadratic increase in conductance was observed when a magnetic field was applied at low temperatures.

Our results will open up a new class of materials for a number of applications. While MXenes have been known to exhibit many favorable properties for applications, briefly listed in the introduction, above,<sup>17,19–29</sup> little is known about single layer flakes. Our temperature-dependent measurements clearly show that  $\text{Ti}_3\text{C}_2\text{-MXene}$  maintains its metallic property even down to the monolayer level. This makes it an attractive material for TCF (transparent conductive film) applications, in particular, since both titanium and carbon are non-toxic, relatively inexpensive, and earth abundant elements. The metallic nature of monolayer  $\text{Ti}_3\text{C}_2\text{T}_x$  is also of great importance for its application in supercapacitors,<sup>18,22,23</sup> where a good conductivity at the highest possible surface-to-mass ratio is a prerequisite ( $\text{Ti}_3\text{C}_2\text{T}_x$  has an estimated specific surface area of  $517 \text{ m}^2/\text{g}$  (Ref. 37)). Furthermore, we demonstrated that the electronic properties of single layer  $\text{Ti}_3\text{C}_2\text{T}_x$  can be tuned using the field-effect. This, together with the above mentioned properties, opens up a wide variety of applications in thin-film electronics. While in the present study, the field effect was small, our results serve as a “proof of principle.” However, they allowed us to deduce the previously unknown carrier densities and mobilities of  $\text{Ti}_3\text{C}_2\text{T}_x$ , two fundamental properties. Finally, we would like to point out that the surface termination groups will have significant effects on the work function and electrical properties

of these new compounds.<sup>32,33,38</sup> Therefore, tailored surface termination groups may be used to adjust the carrier density and bring it down into the range of those of typical conventional (silicon based) or exploratory (graphene) field-effect devices.

We wish to thank Sebastian Küpper for sharing his annealing system and Dr. Martin P. Geller for fruitful discussions. This work was partially funded by the Ceramics program of the Division of Materials Research of the National Science Foundation (DMR-1310245).

- <sup>1</sup>K. S. Novoselov, A. K. Geim, S. V. Morozov, D. Jiang, Y. Zhang, S. V. Dubonos, I. V. Grigorieva, and A. A. Firsov, *Science* **306**, 666 (2004).
- <sup>2</sup>A. C. Ferrari, F. Bonaccorso, V. Fal'ko, K. S. Novoselov, S. Roche, P. Bøggild, S. Borini, F. H. L. Koppens, V. Palermo, N. Pugno, J. A. Garrido, R. Sordan, A. Bianco, L. Ballerini, M. Prato, E. Lidorikis, J. Kivioja, C. Marinelli, T. Ryhänen, A. Morpurgo, J. N. Coleman, V. Nicolosi, L. Colombo, A. Fert, M. Garcia-Hernandez, A. Bachtold, G. F. Schneider, F. Guinea, C. Dekker, M. Barbone, Z. Sun, C. Galiotis, A. N. Grigorenko, G. Konstantatos, A. Kis, M. Katsnelson, L. Vandersypen, A. Loiseau, V. Morandi, D. Neumaier, E. Treossi, V. Pellegrini, M. Polini, A. Tredicucci, G. M. Williams, B. Hee Hong, J. Ahn, J. Min Kim, H. Zirath, B. J. van Wees, H. van der Zant, L. Occhipinti, A. Di Matteo, I. A. Kinloch, T. Seyller, E. Quesnel, X. Feng, K. Teo, N. Rupasinghe, P. Hakonen, S. R. T. Neil, Q. Tannock, T. Löfwander, and J. Kinaret, *Nanoscale* **7**, 4598 (2015).
- <sup>3</sup>L. Ci, L. Song, C. Jin, D. Jariwala, D. Wu, Y. Li, A. Srivastava, Z. F. Wang, K. Storr, L. Balicas, F. Liu, and P. M. Ajayan, *Nat. Mater.* **9**, 430 (2010).
- <sup>4</sup>A. M. van der Zande, P. Y. Huang, D. A. Chenet, T. C. Berkelbach, Y. You, G. H. Lee, T. F. Heinz, D. R. Reichman, D. A. Muller, and J. C. Hone, *Nat. Mater.* **12**, 554 (2013).
- <sup>5</sup>A. Allain and A. Kis, *ACS Nano* **8**, 7180 (2014).
- <sup>6</sup>M. Naguib, V. N. Mochalin, M. W. Barsoum, and Y. Gogotsi, *Adv. Mater.* **26**, 992 (2014).
- <sup>7</sup>M. W. Barsoum, D. Brodtkin, and T. El-Raghy, *Scr. Metall. Mater.* **36**, 535 (1997).
- <sup>8</sup>M. W. Barsoum, *MAX Phases: Properties of Machinable Ternary Carbides and Nitrides* (Wiley-VCH, 2013).
- <sup>9</sup>P. Eklund, M. Beckers, U. Jansson, H. Höüberg, and L. Hultman, *Thin Solid Films* **518**, 1851 (2010).
- <sup>10</sup>M. Radovic and M. W. Barsoum, *Am. Ceram. Soc. Bull.* **92**, 20 (2013); available at [http://ceramics.org/wp-content/uploads/2013/03/bulletin042013\\_maxphases.pdf](http://ceramics.org/wp-content/uploads/2013/03/bulletin042013_maxphases.pdf).
- <sup>11</sup>M. W. Barsoum, *Prog. Solid State Chem.* **28**, 201 (2000).
- <sup>12</sup>M. W. Barsoum and T. El-Raghy, *Metall. Mater. Trans. A* **30**, 363 (1999).
- <sup>13</sup>M. Radovic, M. W. Barsoum, T. El-Raghy, and S. M. Wiederhorn, *J. Alloys Compd.* **361**, 299 (2003).
- <sup>14</sup>M. Magnuson, O. Wilhelmsson, J.-P. Palmquist, U. Jansson, M. Mattesini, S. Li, R. Ahuja, and O. Eriksson, *Phys. Rev. B* **74**, 195108 (2006).
- <sup>15</sup>M. Naguib, M. Kurtoglu, V. Presser, J. Lu, J. Niu, M. Heon, L. Hultman, Y. Gogotsi, and M. W. Barsoum, *Adv. Mater.* **23**, 4248 (2011).
- <sup>16</sup>J. Halim, K. M. Cook, M. Naguib, P. Eklund, Y. Gogtsi, J. Rosen, and M. W. Barsoum, *Appl. Surf. Sci.* **362**, 406 (2016).
- <sup>17</sup>M. Naguib, J. Come, B. Dyatkin, V. Presser, P.-L. Taberna, P. Simon, M. W. Barsoum, and Y. Gogotsi, *Electrochem. Commun.* **16**, 61 (2012).
- <sup>18</sup>M. R. Lukatskaya, O. Mashtalir, C. E. Ren, Y. Dall'Agnese, P. Rozier, P. L. Taberna, M. Naguib, P. Simon, M. W. Barsoum, and Y. Gogotsi, *Science* **341**, 1502 (2013).
- <sup>19</sup>Y. Xie, M. Naguib, V. N. Mochalin, M. W. Barsoum, Y. Gogotsi, X. Yu, K.-W. Nam, X.-Q. Yang, A. I. Kolesnikov, and P. R. C. Kent, *J. Am. Chem. Soc.* **136**, 6385 (2014).
- <sup>20</sup>X. Liang, A. Garsuch, and L. F. Nazar, *Angew. Chem., Int. Ed.* **54**, 3907 (2015).
- <sup>21</sup>D. Er, J. Li, M. Naguib, Y. Gogotsi, and V. B. Shenoy, *ACS Appl. Mater. Interfaces* **6**, 11173 (2014).
- <sup>22</sup>M. Ghidui, M. R. Lukatskaya, M.-Q. Zhao, Y. Gogotsi, and M. W. Barsoum, *Nature (London)* **516**, 7529 (2014).
- <sup>23</sup>X. Wang, S. Kajiyama, H. Iinuma, E. Hosono, Sh. Oro, I. Moriguchi, M. Okubo, and A. Yamada, *Nat. Commun.* **6**, 6544 (2015).

- <sup>24</sup>X. Xie, S. Chen, W. Ding, Y. Nie, and Z. Wei, *Chem. Commun.* **49**, 10112 (2013).
- <sup>25</sup>O. Mashtalir, K. M. Cook, V. N. Mochalin, M. Crowe, M. W. Barsoum, and Y. Gogotsi, *J. Mater. Chem. A* **2**, 14334 (2014).
- <sup>26</sup>J. Chen, K. Chen, D. Tong, Y. Huang, J. Zhang, J. Xue, Q. Huang, and T. Chen, *Chem. Commun.* **51**, 314 (2015).
- <sup>27</sup>H. Liu, C. Duan, C. Yang, W. Shen, F. Wang, and Zh. Zhu, *Sens. Actuators, B* **218**, 60 (2015).
- <sup>28</sup>J. Halim, M. R. Lukatskaya, K. M. Cook, J. Lu, C. R. Smith, L. Naslund, S. J. May, L. Hultman, Y. Gogotsi, P. Eklund, and M. W. Barsoum, *Chem. Mater.* **26**, 2374 (2014).
- <sup>29</sup>Q. Peng, J. Guo, Q. Zhang, J. Xiang, B. Liu, A. Zhou, R. Liu, and Y. Tian, *J. Am. Chem. Soc.* **136**, 4113 (2014).
- <sup>30</sup>See supplementary material at <http://dx.doi.org/10.1063/1.4939971> for details about MXene production and device fabrication.
- <sup>31</sup>Y. Xie and P. R. C. Kent, *Phys. Rev. B* **87**, 235441 (2013).
- <sup>32</sup>A. D. Dillon, M. Ghidui, A. Krick, J. Griggs, S. J. May, Y. Gogotsi, M. W. Barsoum, and A. T. Fafarman, "Highly-Conductive, Optical-Quality Films from Solution-Processed 2D Titanium Carbide (MXene)" (unpublished).
- <sup>33</sup>I. Shein and A. Ivanovskii, *Comput. Mater. Sci.* **65**, 104 (2012).
- <sup>34</sup>F. F. Fang and W. E. Howard, *Phys. Rev. Lett.* **16**, 797 (1966).
- <sup>35</sup>H. C. P. Movva, A. Rai, S. Kang, K. Kim, B. Fallahzad, T. Taniguchi, K. Watanabe, E. Tutuc, and S. K. Banerjee, *ACS Nano* **9**, 10402 (2015), and references therein.
- <sup>36</sup>T. Ouisse, L. Shi, B. A. Piot, B. Hackens, V. Mauchamp, and D. Chaussende, *Phys. Rev. B* **92**, 045133 (2015).
- <sup>37</sup>O. Mashtalir, M. Naguib, V. N. Mochalin, Y. Dall'Agnese, M. Heon, M. W. Barsoum, and Y. Gogotsi, *Nat. Commun.* **4**, 1716 (2013).
- <sup>38</sup>A. N. Enyashin and A. L. Ivanovskii, *J. Phys. Chem. C* **117**, 13637 (2013).